Mol Cell Biochem
DOI 10.1007/s11010-010-0386-9

Angiostatic effects of K252a, a Trk inhibitor, in murine brain capillary endothelial cells

Shimon Lecht · Hadar Arien-Zakay · Martin Kohan · Peter I. Lelkes · Philip Lazarovici

Received: 7 July 2009 / Accepted: 25 January 2010

Abstract Nerve growth factor (NGF) supports the survival and differentiation of sympathetic and sensory neurons and is also mitogenic for a variety of tumors. K252a, an antagonist of NGF receptor TrkA, was previously used as a pharmacological tool to study NGF actions and as a lead compound for developing anti-tumor drugs. Since recently, NGF was characterized as an angiogenic factor, we sought to investigate the angiostatic properties of K252a on endothelial cells (ECs). For this purpose, we used a murine brain microcapillary ECs model in which we found autocrine release of NGF in the culture medium and activation of TrkA receptor-induced downstream signaling molecules Erk1/2, Akt, and PLCγ. In this model, we demonstrated the angiostatic property of K252a based on its ability to affect several important angiogenic steps. K252a, but not its cell membrane impermeable analogue K252b at 100 nM: (i) inhibited the proliferation of the ECs by 45 ± 9%; (ii) reduced by 70 ± 4% the migration of the ECs measured in a wound-closure model; (iii) reduced by 29 ± 9% the formation of tube-like structures of the ECs cultured on Matrigel; (iv) stimulated by 100 ± 25% the collagen deposition by the ECs, a process responsible for the increased endothelial barrier functions expressed by 22 ± 5% reduction of paracellular permeability and by 17 ± 3% elevation of transendothelial electrical resistance. These data suggest that NGF/TrkA may represent a target for the development of novel, K252a-derived multikinase inhibitors drugs with anti-tumor and angiostatic dual activities.

Keywords K252a · K252b · Angiostatic · Nerve growth factor · TrkA receptor · Signaling

This study is part of the PhD thesis of SL to be submitted to The Hebrew University of Jerusalem.

S. Lecht · H. Arien-Zakay · M. Kohan · P. Lazarovici (✉)
School of Pharmacy-Institute for Drug Research, Faculty of Medicine, The Hebrew University of Jerusalem, POB 12065, Jerusalem 91120, Israel
e-mail: philipl@ekmd.huji.ac.il

P. I. Lelkes
Laboratory of Cellular Tissue Engineering, School of Biomedical Engineering, Science and Health Systems, Drexel University, Philadelphia, PA, USA

Introduction

Angiogenesis is a complex, yet tightly regulated process involving proliferation, migration, and capillary sprouting of vascular endothelial cells (ECs). Angiogenesis is regulated by a variety of angiogenic growth factors and extracellular matrix (ECM) proteins and their cognate receptors. The concept that angiogenesis is essential for tumor growth and metastasis has boosted the interest on anti-angiogenic compounds targeting vascular ECs [1]. Therefore, the search for novel angiogenesis inhibitors and novel mechanisms of their action is a major aspect in tumor chemotherapy. Anti-angiogenesis therapy takes advantage of the neutralization of angiogenic activity of the vascular endothelial growth factors (VEGF) family with monoclonal antibodies and the use of small molecules targeting the activity of their tyrosine kinase receptors [2]. Recent studies, provide evidence for a direct involvement of classical neurotrophins, such as nerve growth factor (NGF) and brain-derived neurotrophic factor (BDNF) in the angiogenic processes [3, 4], in addition to the well established role of angiogenic growth factors, such as VEGF and fibroblast growth factor-2 (FGF-2) [5, 6].

The neurotrophins are a family of growth factors acting on cells of different tissues [7]. As for many other growth

Published online: 11 February 2010

factors, dysregulation of neurotrophins and their receptors expression and activity are found in a number of tumors where they can accompany or contribute to malignant transformation [8] through: (i) initiation of mitogenic signals that facilitate tumor growth [9]; (ii) regulation of cell spreading and metastasis formation [10]; and (iii) promotion of survival of tumor cells [11]. NGF, the prototype growth factor of the neurotrophins family is characterized by multi-directional actions on the nervous, cardiovascular, immune, and other peripheral tissues [12]. NGF was found beneficial in clinical trials for Alzheimer's disease [13], diabetic neuropathies [14], and skin and corneal ulcers [15]. On the other hand, tumors exploit the NGF and its receptors overexpression to assist in their growth [16] and angiogenesis [4]. Therefore, NGF and its receptors are potential targets for cancer therapy and K252a, NGF/TrkA receptor inhibitor, provides an important tool to investigate both the NGF-induced tumor growth as well as NGF-induced tumor angiogenesis.

Neurotrophins and their receptors promote tumor growth by either autocrine or paracrine mechanisms, directly affecting cancer cells and/or by promoting tumor angiogenesis. NGF and its tyrosine kinase receptor, TrkA, are co-expressed in peritumoral and intratumoral blood vessel ECs in serous ovarian carcinoma, together with VEGF and FGF-2 [17] exemplifying the complex autocrine loops in tumor growth. Recent studies characterized NGF as a novel angiogenic factor, promoting proliferation, migration, aortic ring sprouting, and neovascularization [4, 5, 18]. TrkA-mediated pleiotropic effects of NGF in normal and transformed cells have been investigated using the alkaloid K252a as a pharmacological tool [19]. K252a but not its cell membrane impermeable analogue K252b at concentrations between 10 and 1000 nM inhibited NGF-stimulated TrkA receptor phosphorylation and signaling, therefore providing an useful lead compound toward development of novel anti-tumor drugs [11]. K252a has no effect (even at micromolar concentrations) on other tyrosine protein kinases such as the receptors for epidermal growth factor (EGF) and platelet-derived growth factor (PDGF) and the products of the v-src and v-fms oncogenes [20]. However, at high concentrations, K252a also inhibits, a number of serine–threonine kinases such as protein kinase C, protein kinase A, protein kinase G, myosin light chain kinase, calmodulin-dependent kinases, and mixed lineage kinases [21] by ATP competition [19]. K252a is a potent, versatile anti-tumor agent, which directly inhibits the growth of lung adenocarcinoma [22], reduces the ability of gastric carcinoma to form lung metastases [23], suppresses the growth of human endometrium cancer cells [24], and inhibits proliferation of ovarian cancer cells [25]. K252a derivatives, such as CEP-701 are in clinical trials as anti-tumor chemotherapeutic agents [11, 26].

In view of the emerging evidence for the angiogenic activity of neurotrophins [27], we sought to investigate the angiostatic potential of K252a using several in vitro angiogenic models. In this study, we report for the first time that K252a in the nanomolar range, at non-cytotoxic concentrations, exerts angiostatic effects as assessed by the inhibition of ECs proliferation, migration, and tube formation on Matrigel. These angiostatic effects were apparently related to chronic Erk1/2 inhibition. These findings suggest that the anti-tumor effects of K252a in vivo represent a combination of both inhibition of neurotrophin-induced tumor growth as well as angiostatic effects.

Materials and methods

Cell culture

Mouse brain capillary ECs, bEnd.3, were obtained from ATCC (Manassas, VA, USA). bEnd.3 cells were cultured in T75 tissue culture flasks (Nunc, Denmark). The growth medium consisted of Dulbecco's modified Eagle's medium (DMEM) supplemented with 4.5 mg/ml glucose, 10% fetal calf serum (FCS), 2 mM L-glutamine, penicillin 10,000 U/ml, and streptomycin 100 μg/ml (Beit Haemek, Afula, Israel). Confluent cultures were split at 1:10 ratio after trypsinization with 0.25% trypsin solution (Beit Haemek) [28]. PC12 pheochromocytoma cells, which were used for neuronal bioassay, were maintained in culture as previously described [29]. The cell cultures were maintained at 37°C in a humidified incubator in a mixture of 5% CO_2/95% air. The medium was changed every second day. Visual evaluation of the cells was performed using an inverted phase contrast light microscope (Nicon® Eclipse TS-100, Japan).

NGF mRNA expression

Total RNA was isolated from cell cultures using the total RNA isolation kit (Promega, Madison, WI, USA), according to the protocol recommended by the manufacturer. For reverse transcription, 1 μg of total RNA was used with the Reverse Transcription kit (Promega, Madison, WI, USA) according to the manufacturer's protocol. For the RT–PCR reactions GoTaq® Green Master Mix (Promega, Madison, WI, USA) was used. The reactions were carried out with 5 μg cDNA and 70 pmol each of sense and anti-sense primers in a final volume of 30 μl. The following mouse-specific primer pairs were used: (i) NGF sense—TGC TGA ACC AAT AGC TGC C; anti-sense—ATC TCC AAC CCA CAC ACT GAC; product size 271 bp, (ii) β-actin sense—TCA TGA AGT GTG ACG TTG ACA TCC GT; anti-sense—CTT AGA AGC ATT TGC GGT

GCA CGA TG; product size 285 bp. The PCR reactions of NGF were started by denaturation of the mixture for 3 min at 94°C followed by 35 cycles of 30 s at 94°C, 1 min at 60°C, 2 min at 72°C each, and a final extension step of 7 min at 72°C. β-actin was used as a normalization control and started with denaturation for 2 min at 94°C followed by 35 amplification cycles of 30 s at 94°C, 1 min at 65°C, 2 min at 68°C, and a final extension step of 7 min at 68°C. The PCR reactions were performed using Mastercycler gradient instrument (Eppendorf, Germany). The PCR products were separated by electrophoresis (100 V for 40 min) in agarose gel (2%) containing ethidium bromide for UV visualization, as previously described [30].

Estimation of NGF by bioassay, ELISA, and western blotting

Upon reaching 90% confluence, the regular growth medium of the bEnd.3 cultures was replaced with serum-free DMEM medium and the cells were cultured for another 48 h to generate conditioned medium (CM). Thereafter, the CM was collected and filtered through 0.2 μm cellulose acetate filter (Whatman, Germany). The filtered CM was kept at -20°C and was thawed prior to experiments. After collecting the CM, the bEnd.3 monolayers were trypsinized and the number of cells was counted using hemocytometer in order to normalize the concentration of CM per cell number. Samples of CM were evaluated for the capability of inducing neurite outgrowth (neuronal differentiation), using a PC12-based neurotropic bioassay. This bioassay is based on the ability of NGF to induce neurite outgrowths from PC12 cells upon activation of TrkA receptor [29]. Neuronal differentiation expressed by neurite elongation after 3 days of CM treatment of PC12 was quantified from images acquired with a Nikon Coolpix5000 camera mounted on a Nikon Eclipse TS100 microscope at 200× magnification. The positive control in this experiment is represented by measurements of neurite outgrowths induced by 10 ng/ml mouse β-NGF (kindly provided by Alomone Labs, Jerusalem, Israel). The contribution of NGF in the CM is estimated from experiments of inhibition of CM-induced differentiation by the presence of 100 nM K252a. Control cultures were left untreated to estimate the spontaneous neurite outgrowth. The extent of neuronal differentiation was calculated using the D_f parameter, as previously described [29]. A D_f value higher than 0.7 indicates a neutrophic factor-induced neurite outgrowth effect. In parallel, aliquots of the CM were assayed for mouse β-NGF using an NGF-specific, Emax® ImmunoAssay system ELISA kit, according to the manufacturer's instructions (Promega, Madison, WI, USA), as previously described [30]. Detection of NGF in the CM by western blotting was performed using anti-mouse β-NGF rabbit polyclonal antibody (kindly provided by Alomone Labs, Jerusalem, Israel) at a dilution of 1:500.

LDH release-based cell death assay

Cell death after treatment with K252a or K252b (kindly provided by Fermentek Ltd., Jerusalem, Israel) was measured by quantifying the activity of released lactate dehydrogenase (LDH) into the medium, using a commercial kit (Pointe, Canton, MI, USA). LDH activity was determined spectrophotometrically at 340 nm by following the rate of conversion of oxidized nicotinamide adenine dinucleotide (NAD^+) to the reduced form (NADH). Total LDH (extracellular + intracellular) was obtained by freezing and thawing the cultures. The K252a- or K252b-induced cell death was expressed as percentage of released LDH from total LDH activity as previously described [28].

Endothelial cell proliferation

To assess the effects of K252a on ECs proliferation, 2×10^3 cells were added to each well of 96-wells tissue culture plates (Nunc, Denmark) and left to adhere overnight in regular culture medium. Thereafter EC cultures were supplemented with different inhibitors in 1% FCS glucose-containing DMEM with 2 mM L-glutamine, 10,000 U/ml penicillin, and 100 μg/ml streptomycin. After 3 days of treatment cell numbers were estimated using the 3-(4,5-Dimethylthiazol-2-yl)-2,5-diphenyltetrazolium bromide (MTT) assay according to the manufacturer's instructions (Sigma, Jerusalem, Israel). Briefly, MTT was added to the wells at a final concentration of 0.5 mg/ml for 40 min. At the end of the incubation period, the medium was aspirated and the cell monolayer was solubilized with DMSO. The optical density (OD) of the solution was measured at 570 nm using a FluorPlus spectrofluorimeter (Tecan, Switzerland). The change in cell number upon K252a or K252b treatment was expressed as percentage change in OD compared to control cells (treated with 0.01% DMSO used to dissolve the inhibitors) [28]. In alternative experiments to generate growth curves the proliferation was measured using Alamar blue reagent (AbD Serotec, Raleigh, NC, USA) as previously described [29]. The proliferation of bEnd.3 cells was estimated every second day over a period of 6 days upon incubation at each time point of the cultures for 4 h with the Alamar blue (10% v/v in complete medium). At the end of the incubation period, media samples were collected and their fluorescence intensity was evaluated in an ELISA reader (Tecan, Switzerland) at an excitation of 560 nm and emission of 595 nm at constant gain. The cell proliferation is presented as the increase in Alamar Blue fluorescent intensity expressed by arbitrary units (a.u.).

Endothelial cell migration

Endothelial cell migration was measured using a wound-healing assay [28]. In brief, 1×10^5 cells/well were added to 12-well culture plates and left to adhere overnight. The next day the medium was changed to 1% FCS glucose-containing DMEM with 2 mM L-glutamine, 10,000 U/ml penicillin, and 100 μg/ml streptomycin. Upon formation of a confluent monolayer (after 2 days), cell migration was initiated by scratching the ECs monolayer with a small pipette tip, thus generating a cell-free area (wound) of ~1 mm width. The wounded cultures were washed three times with 1% FCS medium and pictures of the wounds at time 0 h were taken. Thereafter, culture medium with different treatments was added and the cultures were allowed to migrate for 24 h. At the end of the migration experiment, another set of pictures was taken of the same regions. The area of the wounds was quantified using SigmaScan 5.0 program (Systat, Sweden). In order to assess cell migration at the wound edge and to calculate the area covered by migrating cells, the cell-free areas of the "wounds" at 24 h post wounding were subtracted from the area of the wounds at 0 h time point and calculated as a percentage of untreated (control) cultures [28].

Measurements of Erk1/2 phosphorylation by western blotting

Total cellular protein was extracted following lysis of the cells on ice for 30 min using a commercial cell lysis buffer (Cell Signaling Technology, Beverly, MA, USA). Thereafter the lysed cells were centrifuged for 10 min at 14,000 rpm. The supernatant was collected and total protein was quantified using the Bradford reagent assay (Bio-Rad, Hercules, CA, USA). For western blotting, equal amounts of protein were loaded on 10% polyacrylamide gels, separated by SDS–PAGE (100 V for 1.5 h), transferred on ice to nitrocellulose membranes (90 V for 1.5 h) (Whatman, Germany). To minimize non-specific binding, the membranes were incubated for 2 h at room temperature (RT) with 5% non-fat powdered milk in Tris-buffered saline containing 0.1% Tween-20 (TBST). Immunodetection was performed using primary antibodies (1:1,000; Cell Signaling Technology Inc, Beverly, MA, USA) against phospho- or pan- extracellular regulated kinase 1/2 (Erk1/2). With primary antibodies against phospho-Erk1/2 (p-Erk1/2) the membranes were incubated at 4°C overnight. Following incubation, the membranes were washed with TBST three times and then incubated for 1 h at RT with a horseradish-peroxidase-conjugated goat anti-rabbit secondary antibody (1:10,000; Jackson ImmunoResearch, West Grove, PA, USA). The blots were visualized using an ECL reagent (Pierce, Rockford, IL, USA). Thereafter, the same membranes were washed, incubated for 30 min at RT in Restore Western Blot Stripping Buffer (Pierce, Rockford, IL, USA), and then incubated with the anti-pan-Erk1/2 antibody. Films were exposed from 5 to 60 s, developed and scanned in a flat-bed scanner (Epson, Long Beach, CA, USA). Densitometric analysis was performed with the Quantity One 1-D software (Bio-Rad, Hercules, CA, USA). For each band the densitometric values were obtained for the p-Erk1/2 and the pan-Erk1/2 of the same treatment and the same membrane. The background of each film was subtracted and the relative density of p-Erk1/2 was divided by the density of pan-Erk1/2. In order to compare between different treatments, the relative p-Erk1/2 phosphorylation was normalized to the values of untreated (control) cultures. The data are presented as fold of the normalized basal phosphorylation levels [28].

Endothelial tubular morphogenesis

The assay was performed as previously described [31]. Briefly, bEnd.3 cells were plated on Matrigel (BD, San Jose, CA, USA)-coated wells of a 96-well plate at a density of 2.25×10^4 cells per well in regular growth medium without serum. To record endothelial cell tube formation, wells were photographed 4 h after plating at 200× magnification using a Nikon Coolpix5000 camera mounted on a Nikon Eclipse TS100 microscope. The cumulative tube length was measured using SigmaScan 5.0 (Systat, Sweden). The results are expressed as total length in μm units.

Collagen deposition

In order to quantify the amount of collagen deposited into the subendothelial basement membrane, 5×10^4 bEnd.3 cells per well were plated in 24-well plates. Upon reaching 80% confluence, the cells were treated with different concentrations of K252a for 48 h. Thereafter, the cells were solubilized according to previously described procedure without affecting the extracellular proteins deposited on the bottom of the well [32, 33]. Briefly, the medium was aspirated and the cells were washed once with PBS. Thereafter, each well was incubated for 10 min with 0.5 ml of 0.04 M NH_4OH solution and then the solution was aspirated. In order to remove remaining ammonia and cellular debris the wells were washed 10 times with 0.5 ml PBS. Total collagen (types I–IV) deposited in each well was measured using the Sircol Collagen Assay kit (Biocolor Ltd., United Kingdom) according to the manufacturer's instructions as described previously [34]. Results are presented as fold increase over untreated (control) cells.

Endothelial monolayer integrity: TEER and permeability

For measuring trans-endothelial electrical resistance (TEER) and monolayer permeability, bEnd.3 cells were cultured in double-chamber plates composed of inserts with 1 μm pore-diameter porous polyethylene terephthalate membrane placed inside a 12-well plate (BD Falcon, San Jose, CA, USA). Initially the cells were plated at a density of 5×10^4 cells/insert and were cultured for 5 days to confluence as was verified using phase contrast microscopy observations. The resistance was evaluated using EVOM^{TM} ohmmeter and EndOhm^{TM} chamber (WPI, Sarasota, FL, USA), according to the manufacturer's instructions. For calculating TEER values, the resistance of a blank insert (without cells) was subtracted from that of the cell-containing inserts and the value was multiplied by the area of insert thus generating a resistance values per area (Ohm $\times$ cm^2).

For permeability measurements, the double-chamber plates were washed three times with Ringer's solution (NaCl—111.5 mM; KCl–4.8 mM; $NaHCO_3$–29.2 mM; NaH_2PO_4–0.75 mM; $CaCl_2$*$2H_2O$–1.04 mM; MgCl*$6H_2O$ –0.74 mM; D-glucose—5 mM; pH 7.4). Fluorescein (M_w = 300 Da) or fluorescein-labeled bovine serum albumin (BSA-FITC) (M_w = 66 kDa) (Molecular Probes, Carlsbad, CA, USA) was loaded into the inserts (upper compartment). The concentrations of the fluorescent markers were chosen from the linear part of calibration curve (intensity of fluorescence vs. amount). At different time points, aliquots of 100 μl were collected from the bottom compartment and transferred to the well of 96-well black (low intrinsic fluorescence) plate (Nunc, Denmark). Fluorescence readings were performed using SPECTRAFluorPlus ELISA reader (Tecan, Switzerland) set at 485 nm (excitation) and 535 nm (emission). In order to quantify the fluorescence units each experiment was accompanied with appropriate calibration. To quantify the permeability of markers through the EC monolayers, the P_{app} (apparent permeability) values were calculated using the following equation $P_{app} = dQ/dt/(A \times Cd \times 60)$, where dQ/dt—a slope generated from the linear portion of plotting the accumulating amount of compound in the lower compartment vs. time; A—the effective growth area of the insert's membrane; Cd—the concentration in the insert compartment; 60—conversion factor from minutes to seconds. P_{app} represents a permeability value that consists of both monolayer and insert membrane permeabilities. For calculating the permeability of endothelial monolayer only, the P_{app} values were placed in the following equation, $1/P_e = 1/P_{app}\text{-}1/P_f$, where P_{app}—the total permeability through both insert membrane and cell monolayer; P_f—the permeability through the insert membrane only; P_e—the permeability value through endothelial monolayer only [35].

Statistics

The results are presented as the mean ± SD or SEM of at least three independent experiments and were evaluated using the InStat3 statistics program (GraphPad, La Jolla, CA, USA). Statistically significant differences between experimental groups were determined by analysis of variance (ANOVA) with Bonferroni post-hoc test and considered significant when $P < 0.05$.

Results

NGF expression and signaling in brain capillary endothelial cells

Brain capillary endothelial cells, bEnd.3, express mRNA transcripts for NGF as found in the mouse brain (Fig. 1a—upper insert) and release NGF into the medium as visualized by the western blotting experiment in Fig. 1a—lower insert). To further confirm and quantify NGF level in the CM we performed an NGF-specific ELISA assay (Fig. 1a). This assay clearly indicates the presence of 31 ± 3 pg/ml of NGF in the CM (indicating a rate of secretion of 223 ± 12 pg NGF/10^6 cells/day). In parallel experiments, using a PC12-based neuronal bioassay [29] as independent mean of validation, we measured the CM-induced neurotropic effect (neuronal differentiation expressed by neurites outgrowths of cells). This bioassay is specific for NGF with no neurotropic response to BDNF, neurotrophin-3, neurotrophin-4, glial-derived neurotrophic factor, ciliary neurotrophic factor, human leukemia inhibiting factor [36], and VEGF [37]. In this bioassay, NGF but not FGF-2 neurotropic effect is blocked by K252a [36, 37]. In order to measure the amount of NGF released into bEnd.3-CM, the PC12 cells were exposed to CM, resulting with positive neurotropic effects equivalent to 175 ± 15 pg NGF/10^6 cells/day (Fig. 1b). The effect of CM in the bioassay was inhibited by K252a but not K252b (data not shown) indicating that the neurotropic effect was mainly due to bioactive NGF (Fig. 1b). These findings support the concept that brain capillary ECs synthesize and release bioactive NGF, as previously also documented for BDNF released from bEnd.3 cells [38].

Both NGF receptors TrkA and p75^{NTR} are expressed by bEnd.3 cells [28, 38]; therefore, we hypothesized that release of endogenous NGF as emphasized in Fig. 1 will stimulate the TrkA-established signaling pathways Erk1/2, Akt, and PLCγ [39] in an autocrine fashion. Indeed, naive cultures indicate low basal phosphorylation of all three

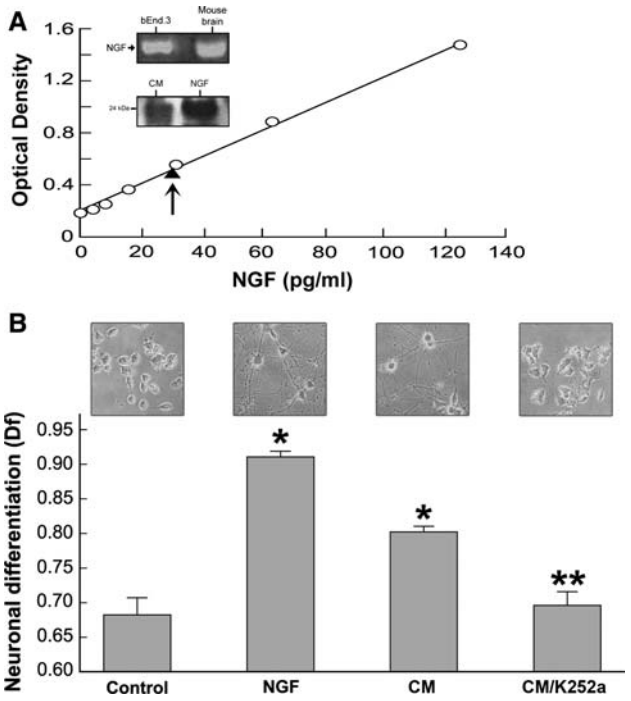

Fig. 1 Brain capillary endothelial cells express and release bioactive NGF. **a** A calibration curve was generated using mouse β-NGF in a range of 0–120 pg/ml (*open circles*). The concentration of NGF in the CM (*arrow–black triangle*) was estimated by extrapolation from the standard curve. Upper insert—bEnd.3 expresses mRNA encoding NGF similar to mouse brain extract that was detected using RT–PCR. Lower insert—western blotting of a CM sample as well as 10 ng of mouse β-NGF were separated by 12% SDS–PAGE, electro-transferred and immunoblotted with mouse β-NGF selective antibody. **b** PC12 cultures were treated with 50% CM in the presence or absence of 100 nM K252a in comparison to 10 ng/ml NGF or left untreated (Control). The level of NGF in CM based on the bioassay measurements was estimated by D_f as described in "Materials and methods" section. Data are the mean ± SEM of four independent experiments ($n = 10$–12). * $P < 0.01$ vs. control, ** $P < 0.05$ vs. CM. Upper micrographs of selected cultures visualize the extent of neuronal differentiation

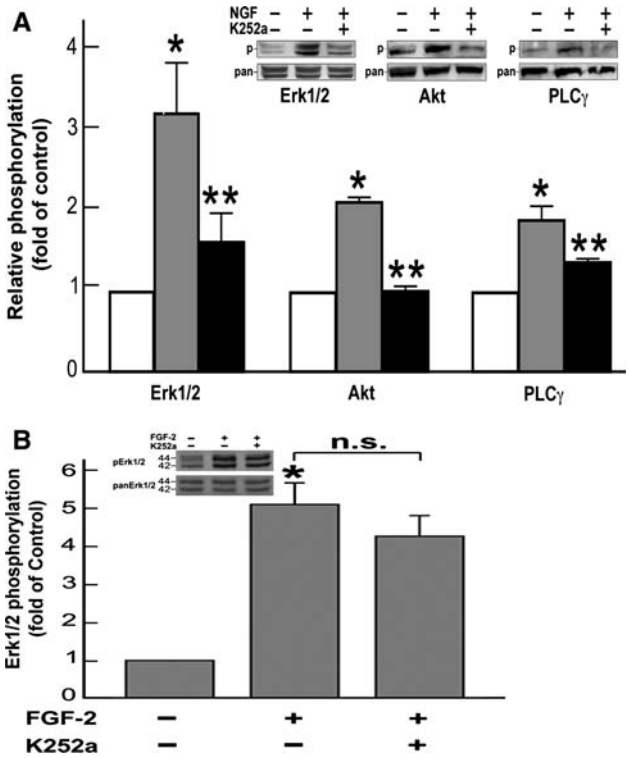

Fig. 2 NGF-induced signaling in bEnd.3 cells is inhibited by TrkA receptor antagonist, K252a. **a** The cells were treated with NGF (10 ng/ml) for 10 min in the presence or absence of K252a (200 nM). Thereafter, the cells were harvested, lysed, and submitted for western blotting to measure the Erk1/2, Akt, and PLCγ phosphorylation (p) and unphosphorylated proteins (pan). Upper part—Representative pictures of western blotting analysis. Lower part—Quantization of phosphorylation relative to control cells as described in "Materials and methods" section. Data are the mean ± SD of four independent experiments ($n = 8$–12) * $P < 0.05$ vs. control (0 nM K252a and 0 ng/ml NGF), ** $P < 0.05$ vs. NGF. **b** The lack of inhibition by K252a on FGF-2-induced Erk1/2 phosphorylation. The cells were treated with FGF-2 (10 ng/ml) for 10 min in the presence or absence of K252a (200 nM). Thereafter, the cells were harvested, lysed, and submitted for western blotting to measure the Erk1/2 phosphorylation (p) and unphosphorylated proteins (pan). Inserts—Representative pictures of western blotting analysis. Data are the mean ± SD of three independent experiments ($n = 4$–6) * $P < 0.01$ vs. control (0 nM K252a and 0 ng/ml FGF-2), n.s.—not significant

signaling molecules (Fig. 2a). To confirm that NGF can stimulate all these pathways, bEnd.3 cells were treated with an optimal concentration of 10 ng/ml NGF for 10 min in the presence or absence of 200 nM K252a (Fig. 2a). As expected, exposure to NGF, increased by 3.1 ± 0.6, 2.1 ± 0.1, and 1.8 ± 0.1 fold the phosphorylation of Erk1/2, Akt, and PLCγ, respectively. Treatment with NGF in the presence of K252a reduced by 50 ± 9, 47 ± 8, and 28 ± 3% the phosphorylation of Erk1/2, Akt, and PLCγ compared to NGF stimulation, respectively. To confirm the selectivity of K252a inhibition of NGF-induced TrkA signaling, we measured its effect on FGF-2-induced phosphorylation of Erk1/2 in bEnd.3 cells (Fig. 2b). It is evident that FGF-2-induced Erk1/2 phosphorylation in the cells and that pre-treatment with 200 nM K252a lacked a significant inhibitory effect. These findings support the notion that NGF-induced phosphorylation of the signaling molecules in bEnd.3 cells is mediated by TrkA.

K252a, but not K252b, inhibits proliferation, migration, and tube formation

K252a and K252b are cytotoxic to a variety of cells [19]. As seen in Fig. 3a, 1 h exposure of bEnd.3 cells to both these compounds did not show any cytotoxicity up to a concentration of 400 nM indicating that during the time-period of K252a treatment it was devoid of cytotoxicity. bEnd.3 cells treatment for 72 h with concentration of 400 nM K252a, but not K252b, caused a 20% decrease in

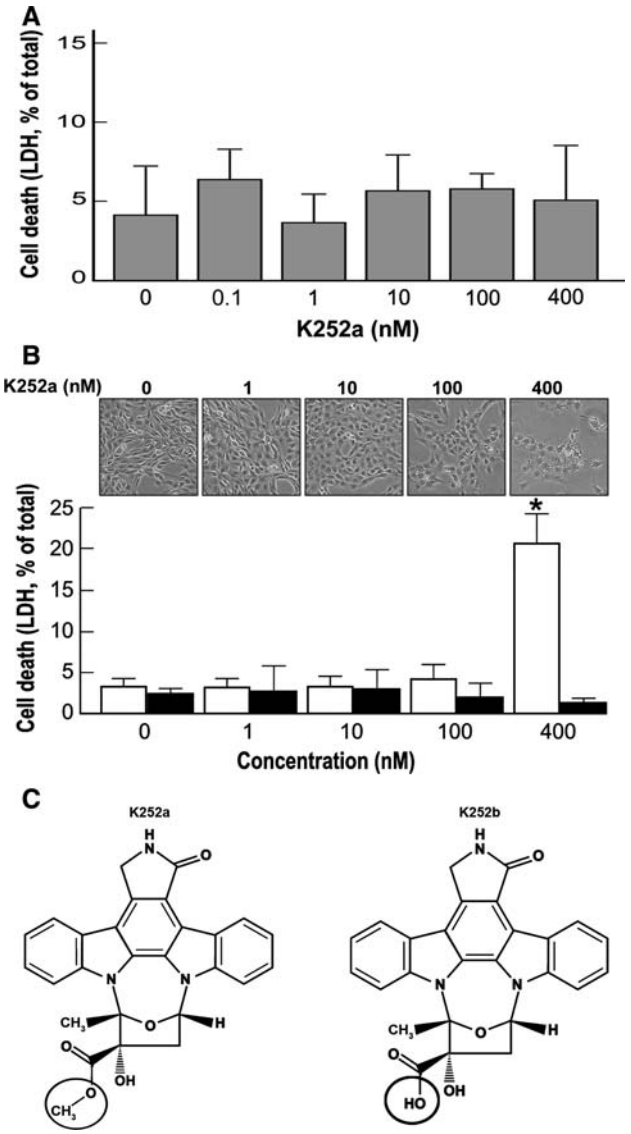

Fig. 3 Viability of bEnd.3 cells upon treatment with K252a analogues. **a** Cell death of cultures treated for 1 h with increasing concentrations of K252a was measured by LDH release to the medium. Data are mean ± SEM of three independent experiments ($n = 9$–12). **b** Cell death of cultures treated for 72 h with increasing concentrations of K252a (*white bars*) and the cell impermeable analogue K252b (*black bars*) was measured by LDH release to the medium. Insert—light microscopical micrographs (200×) of bEnd.3 cultures treated with the indicated concentrations (nM) of K252a. Data are mean ± SEM of three independent experiments ($n = 9$–12). $P < 0.01$ vs. control (0 nM K252a). **c** The chemical structures of K252a (*left*) and K252b (*right*) differ in the side chain of the lactone ring as indicated by *circle*

cell viability (Fig. 3b). At concentrations higher than 400 nM both compounds increased cell death higher than 20% (data not shown). Therefore, in the angiogenic experiments lasting longer than 24 h the concentration of K252a was up to 100 nM. A microscopic evaluation of bEnd.3 cultures exposed to increasing concentrations of K252a revealed significant morphological changes (Fig. 3b—insert) from a cobblestone shape to a more round phenotype [40]. K252b the membrane impermeable analog of K252a, differing in structure by an hydroxyl instead of methyl group in K252a side chain (Fig. 3c), was not toxic at all concentrations investigated (Fig. 3a, b). K252b had no effect on the morphology of bEnd.3 cells.

The effects of K252a and K252b on bEnd.3 proliferation were measured for a period of 3 days at different concentrations of the antagonists (Fig. 4a). K252a at the concentrations between 50 and 400 nM caused a dose-dependent inhibition of cell proliferation in the range of 40–70%. In contrast, K252b caused a slight inhibition of cell growth, and that only at the highest concentrations used (>200 nM). In another approach, the inhibitory effect of 100 nM K252a but

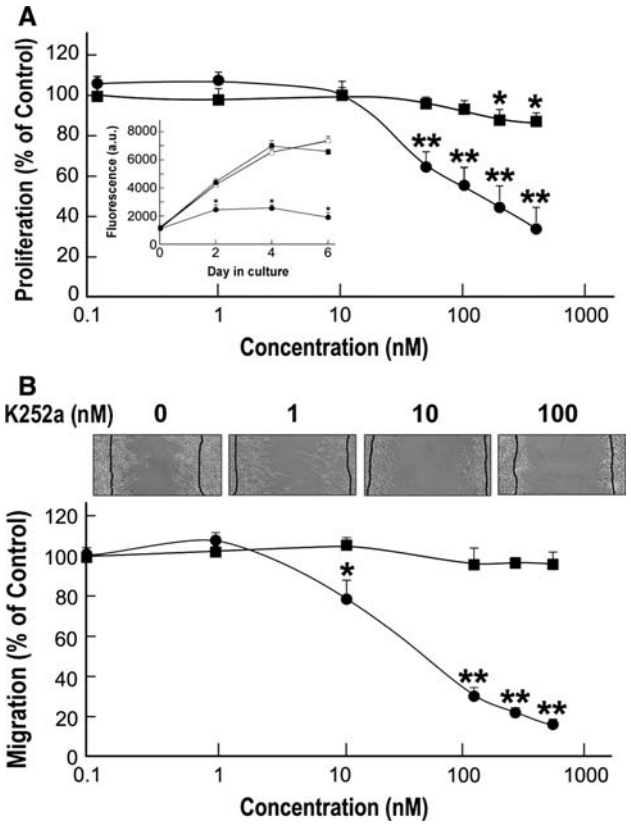

Fig. 4 The inhibitory effects of K252a analogues on proliferation and migration of bEnd.3 cells. **a** Dose-dependent effect of K252a and K252b on cell proliferation at an end-point of 72 h. Insert—the effect of 100 nM K252a or 100 nM K252b on bEnd.3 cells proliferation during a period of 6 days. **b** Dose-dependent effect of K252a and K252b on cell migration using wound-closure assay at an end-point of 24 h. Insert—light microscopical micrographs (100×) of the culture 24 h after wounding. Confluent monolayers were scrapped generating a cell-free strip of about 1 mm (*black lines*) and treated with K252a or K252b with different concentrations or left untreated. K252a—*black circles*; K25b—*black squares*. Data are mean ± SEM of three independent experiments ($n = 9$–12). * $P < 0.05$ and ** $P < 0.01$ vs. control (0 nM)

not 100 nM K252b is evident from the bEnd.3 growth curve during a time-period of 6 days (Fig. 4a—insert).

The effects of K252a and K252b on bEnd.3 migration were measured for a period of 24 h at different concentrations using a wound-closure model, as described in the "Material and methods" section. K252a at concentrations between 10 and 400 nM inhibited ECs migration in a dose-dependent fashion (20–85%), while K252b had no significant effect on migration (Fig. 4b). Since 10 nM K252a inhibits bEnd.3 cells migration (Fig. 4b) while not affecting proliferation (Fig. 4a), we conclude that the anti-migratory effect of K252a is not due to a decrease in cell proliferation. The inhibitory effects of K252a on both proliferation and migration of bEnd.3 cells (Fig. 4) maybe explained by the inhibition of the autocrine released NGF. To verify this possibility the effect of CM on bEnd.3 proliferation and migration was investigated and the inhibitory effect of K252a on these cellular processes was characterized (Fig. 5). CM induced an increase of about 70% in proliferation and migration of the cells, effects that were K252a-inhibited by 50 and 60%, respectively. The residual CM-induced proliferation and migration effects, which were not affected by K252a, may reflect the contribution of other angiogenic growth factors present in CM. Exogenous treatment of bEnd.3 cells with 10 ng/ml NGF induced an increase of 17 and 10% in proliferation and migration of the cells, respectively, which were completely abolished by K252a. The selective inhibitory effect of K252a on NGF stimulation of proliferation and migration is also supported by the lack of K252a inhibitory effect on FGF-2-stimulated proliferation and migration of bEnd.3 cells (Fig. 5a, b). Altogether, these results support the conclusion that K252a inhibitory effects are specific toward the autocrinally mediated NGF-induced proliferation and migration.

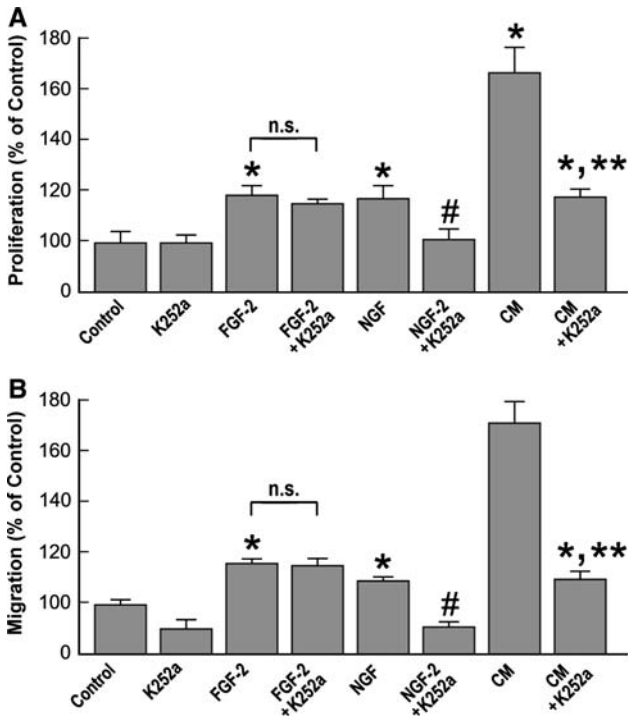

Fig. 5 Characterization of CM-induced proliferation and migration of bEnd.3 cells. bEnd.3 cells proliferation after 72 h of treatment using MTT dye assay (**a**) and migration after 24 h using wound-closure assay (**b**) were measured upon treatment with 50% CM or 10 ng/ml NGF or 10 ng/ml FGF-2 in the presence or absence of 10 nM K252a. Data are mean ± SD of three independent experiments ($n = 9$–12). * $P < 0.05$ vs. Control, # $P < 0.05$ vs. NGF, and ** $P < 0.01$ vs. CM; n.s.—non-significant

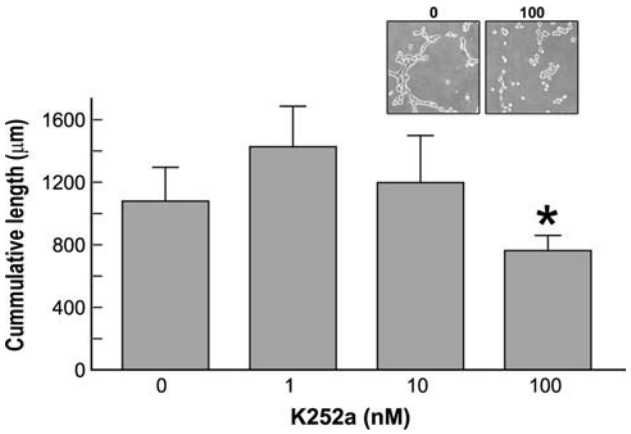

Fig. 6 The inhibitory effects of K252a on tube-like structures formation by bEnd.3 cells on Matrigel. The cumulative length of the tubes (μm) is presented as mean ± SEM of three independent experiments ($n = 6$–9). * $P < 0.05$ vs. control (0 nM). Insert—light microscopical micrograph (200×) of tubular morphogenesis (0 nM) and prevention of "capillary-like" formation by K252a (100 nM)

Like other ECs, bEnd.3 cells cultured on Matrigel formed tube-like structures after 4 h (Fig. 6—insert). K252a at 100 nM inhibits the formation of tubular morphogenesis (Fig. 6—insert), reducing the overall tube length by 28% after 4 h and more pronounced (>70%) after 24 h (data not shown). The inhibitory effect of K252a on "capillary-like" formation on Matrigel may be related to its inhibitory effect on bEnd.3 cell migration (Fig. 4b), thus preventing cell organization into tube-like structure.

K252a-induced long-term inhibition of Erk1/2 phosphorylation

The Erk signaling cascade is critical to the trophic actions of NGF and other growth factors [41]. To investigate whether K252a-induced inhibition of proliferation, migration, and tube formation is correlated with Erk1/2 phosphorylation, bEnd.3 cells were exposed to several concentrations of K252a, lysed and Erk1/2 phosphorylation was assessed, 1 and 72 h following K252a application. As seen in Fig. 7, treatment of the cells for 1 h with 1, 10, and

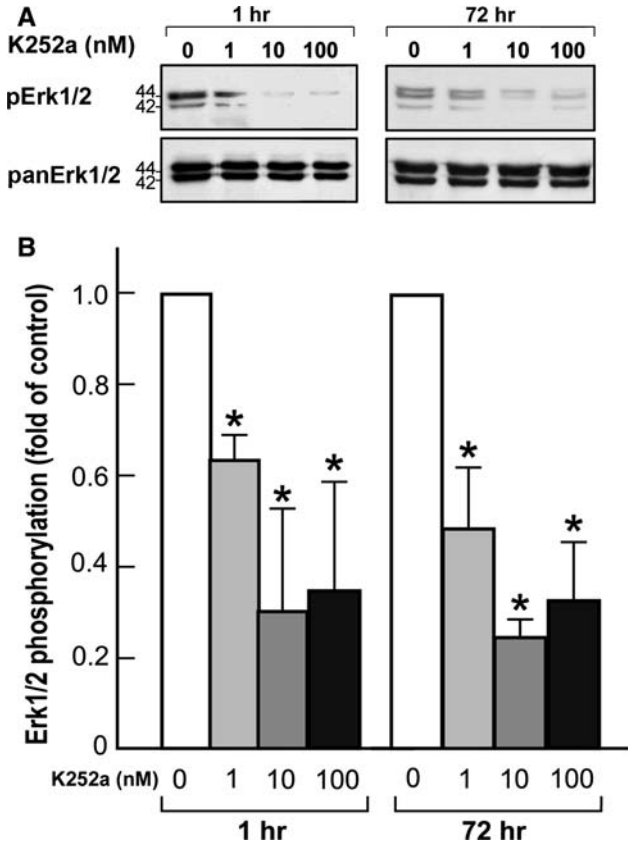

Fig. 7 The dose- and time-dependent inhibitory effects of K252a on Erk1/2 phosphorylation in bEnd.3 cultures. The cells were harvested, lysed, and submitted for western blotting to measure the Erk1/2 phosphorylation (pErk1/2) and unphosphorylated proteins (panErk1/2). **a** Representative pictures of western blotting. **b** Erk1/2 phosphorylation data are the mean ± SD of four independent experiments ($n = 4$–5) * $P < 0.05$ vs. control (0 nM K252a)

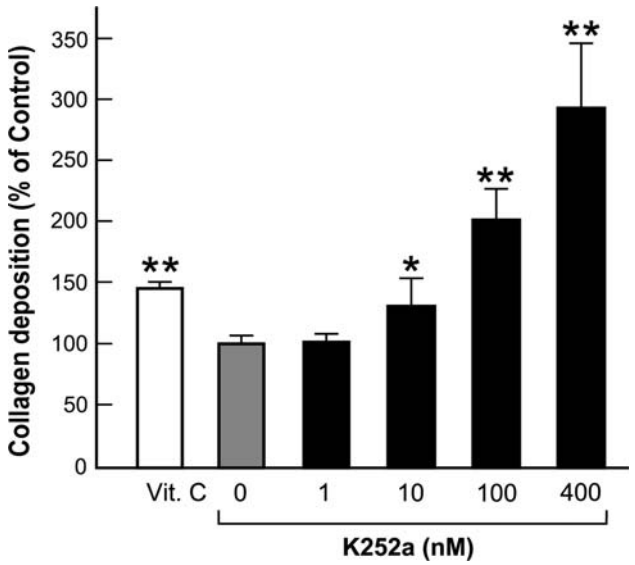

Fig. 8 Dose-dependent effect of K252a on collagen deposition by bEnd.3 cells. The cultures were treated with different concentration of K252a (*black*), vitamin C (*white*, 30 μg/ml) or left untreated (*gray*, 0 nM K252a). The amount of deposited collagen on the well was measured using collagen-specific dye and the data as percentage of control are expressed as mean ± SD of three different experiments ($n = 9$–12). * $P < 0.05$ vs. control (0 nM K252a), ** $P < 0.01$ vs. control (0 nM K252a)

100 nM K252a inhibited Erk1/2 phosphorylation by 37 ± 6, 70 ± 20, and 65 ± 24%, respectively, as compared to control untreated cells. The inhibition of Erk1/2 phosphorylation following exposure for 72 h (51 ± 12, 75 ± 3, and 67 ± 12% for 1, 10, and 100 nM K252a, respectively) was statistically indistinguishable from that for the short-time treatment. The long-term inhibitory effect of K252a on basal activation of Erk1/2 may reflect the contribution of the autocrine-released NGF to TrkA-mediated Erk1/2 phosphorylation in bEnd.3 cells.

K252a-induced deposition of collagen

In view of the important role of extracellular matrix proteins on endothelial barrier properties [42] we measured the effect of K252a treatment on total collagen deposition by the cells as presented in Fig. 8. As positive control we used, vitamin C (ascorbic acid), an established co-factor for hydroxylation of proline and lysine residues in collagen, which increases both the rate of transcription and stability of collagen mRNA resulting in increased total deposition in ECs [43, 44]. K252a from 10 to 400 nM in a dose-dependent fashion increased total collagen deposition from 30 to 160%. Vitamin C (30 μg/ml) increased by 50% total collagen deposition by the bEnd.3 cells.

K252a-induced increase in TEER and reduced paracellular permeability

Since increased collagen deposition was reported to decrease ECs permeability [45] we analyzed the effects of K252a on bEnd.3 monolayer integrity by measuring TEER values and paracellular permeability, as described in the "Materials and methods" section. Treatment of the cells with 100 nM K252a resulted in a small, but statistically significant increase in TEER by 17% (Fig. 9). Consistent with this finding, the permeabilities of fluorescein and BSA were decreased in the presence of K252a by 25 and 50%, respectively (Fig. 9—insert). These findings indicate K252a-induced barrier-stabilizing effects (increased tightness of the monolayer) in bEnd.3 cells. Furthermore, these findings support an apparent correlation between K252a-induced increase in collagen deposition and enhancement of endothelial barrier functions, as also previously reported with bovine aortic and venous ECs [45].

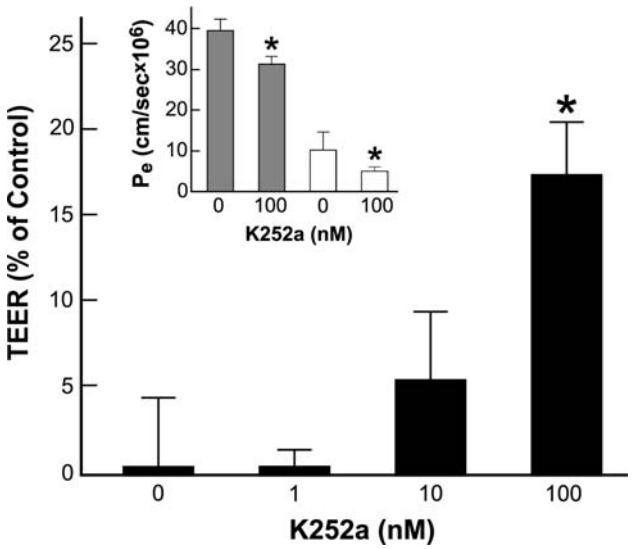

Fig. 9 K252a increased barrier properties of bEnd.3 cell monolayers. TEER of bEnd.3 cultures treated with K252a was measured as described in "Materials and methods" section. Results are expressed as mean ± SD of change in TEER compared with untreated monolayers (0 nM). Insert—effect of K252a on fluorescein (*gray bars*) and BSA (*white bars*) permeabilities through endothelial monolayer. Permeability (P_e) was calculated as described in "Material and methods" section. Data are mean ± SD of three different experiments ($n = 6$–9). * $P < 0.05$ vs. control (0 nM K252a)

Discussion

In the present study, we showed that K252a, an established NGF/TrkA receptor antagonist, might act as a potent angiostatic agent, in addition to its well-known anti-tumor activity [11, 23]. The angiostatic property of K252a is based on its ability to affect series of important angiogenic steps of microvascular ECs. Using cultured murine brain capillary endothelial (bEnd.3) cells as a model system, we demonstrate here for the first time that K252a, at non-cytotoxic concentrations: (i) inhibits the proliferation of the ECs (Figs. 4, 5); (ii) reduces cell migration (Figs. 4, 5); (iii) impairs tubular morphogenesis (Fig. 6); (iv) enhances endothelial barrier functions, as expressed by an elevation of TEER values due to reduced paracellular permeability (Fig. 9), similar to the ascorbic acid reduction of endothelial permeability, due to enhanced collagen synthesis (Fig. 8) [45]. The collagen synthesized by ECs should act on the cells leading to the contraction of their tight junctions and thus blocking macromolecules diffusion. Collagen proteolysis by metallo-proteases is a critical event during early steps of angiogenesis [46]; therefore, increase in collagen deposition provides another angiostatic characteristic of K252a. In view of the present findings, it seems likely that K252a is an angiostatic compound for microvascular ECs. Although the bEnd.3 cell line is similar to primary dissociated brain capillary ECs in expression of NGF receptors, NGF-induced proliferation, NGF secretion after inflammation and protective effects after ischemia [47, 48], further experiments are required to extend present angiostatic properties of K252a on bEnd.3 cells model to in vivo tumor models and derived blood vessels. While anti-angiogenic molecules block tissue-derived angiogenic growth factor, such as VEGF, angiostatic compounds, such as K252a, modulate molecular targets in ECs, which are essential during angiogenesis [49]. Previous studies had shown that K252a inhibited the contraction of arterial smooth muscle [50], the proliferation of cultured smooth muscle cells from bovine carotid artery [51]. Therefore, together with the present results we hypothesize that K252a may affect the in vivo maturation of the tumor-invading blood vessels by inhibiting both endothelial and smooth muscle cellular components.

Although details of molecular mechanism of K252a angiostatic potential in ECs are at present unknown, it is tempting to hypothesize that these effects might, at least in part, involve inhibition of autocrinally released NGF, activating TrkA-mediated effects. This hypothesis is based on the following findings (i) NGF was synthesized and released by the cells (Fig. 1); (ii) bioactive NGF was detected in the endothelial cell-conditioned medium as evident from a neuronal bioassay (Fig. 1); (iii) the activation of all three established signaling pathways downstream of the TrkA receptor, i.e., Erk1/2, Akt, and PLCγ (Fig. 2), suggesting that at least in part they are TrkA-mediated following NGF released into the medium; (iv) this is also evident from the selective inhibition by K252a of the CM-induced proliferation and migration (Fig. 5); (v) the inhibitory effects of K252a on EC tube formation (hours) (Fig. 6), migration (1 day), and proliferation (3 days) (Fig. 4) are apparently correlated with a long-term inhibition of Erk1/2 phosphorylation (Fig. 7). These latter findings are in line with the concept that suppression of MAPK/Erk signaling pathway is related to the inhibition of proliferation, migration, and tube formation of ECs [52, 53], representing an alternative angiostatic molecular pathway, in addition to the NFκB pathway, which seems to be common to other angiostatic agents [54].

Another possibility to explain the strong angiostatic effects of K252a is a partial contribution of its multikinase inhibition property. Serine–threonine kinases, such as protein kinase C are known to be inhibited by K252a [19], and have been proposed to regulate angiogenesis [55]. Therefore, we surmise that K252a may also affect these kinases, resulting in the observed strong angiostatic effects at high concentrations. The identity of the brain capillary endothelial kinases and their substrates susceptible to inactivation by K252a is presently unknown, as is their involvement in angiogenesis. Because K252b, the cell membrane impermeable analogue of K252a, lacks the

angiostatic effects observed with K252a, it is likely that K252a exerts its angiostatic actions by binding to intracellular targets. The mode of action of K252a; therefore, may require inhibition of specific kinase(s), a possibility deserving further investigation.

In the view of the important role of NGF in tumor biology, several therapeutic strategies maybe considered: (i) neutralization of the NGF using selective monoclonal antibodies in analogy to the present use of anti-VEGF monoclonal antibody bevacizumab (Avastin®) [56]. Indeed the future availability of tanezumab, a recombinant humanized anti-NGF neutralizing monoclonal antibody [57] will provide such a therapeutic tool; (ii) inhibition of NGF/TrkA receptor by K252a and related CEP compounds, as previously found for modern anti-cancer drugs, such as sorafenib [58], sunitinib [59], and nilotinib [60], all of which are currently being used to treat different types of tumors by the virtue of both inhibiting tumor growth and tumor angiogenesis; (iii) a combination therapy including the above mentioned compounds together with classical chemotherapy. Whatever the NGF-based future chemotherapeutic approach will emerge, the mechanisms whereby K252a exerts its angiostatic effects are of interest because of the proven therapeutic potential of K252a-derived CEP compounds in the treatment of prostate carcinoma [11, 61] and of acute myeloid leukemia [26]. Therefore, K252a and related CEP compounds, besides targeting NGF/TrkA receptor and other kinases in tumors, might be found as potent angiostatic compounds resulting with better therapeutic effects.

Acknowledgments This work was supported in part by a grant-in-aid form the Stein Family Foundations (PL and PIL); PL is affiliated and partially supported by the David R. Bloom Center for Pharmacy; and the Dr. Adolf and Klara Brettler Center for Research in Molecular Pharmacology and Therapeutics at The Hebrew University of Jerusalem, Israel; SL is supported by "Eshkol fellowship" from the Israeli Ministry of Science and Technology. The authors would like to acknowledge the help of Mrs. Zehava Cohen for graphics preparation and the constructive remarks of the referees.

References

1. Folkman J (2007) Angiogenesis: an organizing principle for drug discovery? Nat Rev Drug Discov 6:273–286
2. Herbst RS (2006) Therapeutic options to target angiogenesis in human malignancies. Expert Opin Emerg Drugs 11:635–650
3. Calza L, Giardino L, Giuliani A, Aloe L, Levi-Montalcini R (2001) Nerve growth factor control of neuronal expression of angiogenetic and vasoactive factors. Proc Natl Acad Sci USA 98:4160–4165
4. Nico B, Mangieri D, Benagiano V, Crivellato E, Ribatti D (2008) Nerve growth factor as an angiogenic factor. Microvasc Res 75:135–141
5. Lecht S, Puxeddu I, Levi-Schaffer F, Reich R, Davidson B, Schaefer E, Marcinkiewicz C, Lelkes PI, Lazarovici P (2007) Nerve growth factor—a neurotrophin with angiogenic activity. In: Maragudakis M (ed) Angiogenesis: basic science and clinical applications. Transworld Research Network, Kerala, pp 99–113
6. Lazarovici P, Marcinkiewicz C, Lelkes PI (2006) Cross talk between the cardiovascular and nervous systems: neurotrophic effects of vascular endothelial growth factor (VEGF) and angiogenic effects of nerve growth factor (NGF)-implications in drug development. Curr Pharm Des 12:2609–2622
7. Aloe L, Tirassa P, Bracci-Laudiero L (2001) Nerve growth factor in neurological and non-neurological diseases: basic findings and emerging pharmacological prospectives. Curr Pharm Des 7: 113–123
8. Kruttgen A, Schneider I, Weis J (2006) The dark side of the NGF family: neurotrophins in neoplasias. Brain Pathol 16:304–310
9. Singer HS, Hansen B, Martinie D, Karp CL (1999) Mitogenesis in glioblastoma multiforme cell lines: a role for NGF and its TrkA receptors. J Neurooncol 45:1–8
10. Menter DG, Herrmann JL, Marchetti D, Nicolson GL (1994) Involvement of neurotrophins and growth factors in brain metastasis formation. Invasion Metastasis 14:372–384
11. Ruggeri BA, Miknyoczki SJ, Singh J, Hudkins RL (1999) Role of neurotrophin-trk interactions in oncology: the anti-tumor efficacy of potent and selective trk tyrosine kinase inhibitors in pre-clinical tumor models. Curr Med Chem 6:845–857
12. Fiore M, Chaldakov GN, Aloe L (2009) Nerve growth factor as a signaling molecule for nerve cells and also for the neuroendocrine-immune systems. Rev Neurosci 20:133–145
13. Tuszynski MH, Thal L, Pay M, Salmon DP, Hoi Sang U, Bakay R, Patel P, Blesch A, Vahlsing HL, Ho G, Tong G, Potkin SG, Fallon J, Hansen L, Mufson EJ, Kordower JH, Gall C, Conner J (2005) A phase 1 clinical trial of nerve growth factor gene therapy for Alzheimer disease. Nat Med 11:551–555
14. Pittenger G, Vinik A (2003) Nerve growth factor and diabetic neuropathy. Exp Diabesity Res 4:271–285
15. Aloe L, Tirassa P, Lambiase A (2008) The topical application of nerve growth factor as a pharmacological tool for human corneal and skin ulcers. Pharmacol Res 57:253–258
16. Dolle L, El Yazidi-Belkoura I, Adriaenssens E, Nurcombe V, Hondermarck H (2003) Nerve growth factor overexpression and autocrine loop in breast cancer cells. Oncogene 22:5592–5601
17. Davidson B, Reich R, Lazarovici P, Nesland JM, Skrede M, Risberg B, Trope CG, Florenes VA (2003) Expression and activation of the nerve growth factor receptor TrkA in serous ovarian carcinoma. Clin Cancer Res 9:2248–2259
18. Cantarella G, Lempereur L, Presta M, Ribatti D, Lombardo G, Lazarovici P, Zappala G, Pafumi C, Bernardini R (2002) Nerve growth factor-endothelial cell interaction leads to angiogenesis in vitro and in vivo. FASEB J 16:1307–1309
19. Lazarovici P, Matsuda Y, Kaplan D, Guroff G (1997) The protein kinase inhibitors K252a and Staurosporine as modifiers of neurotrophin receptor signal transduction. In: Gutman Y, Lazarovici P (eds) Cellular and molecular mechanisms of toxin action: toxins and signal transduction. Harwood Academic Publishers, Amsterdam, pp 69–93
20. Tapley P, Lamballe F, Barbacid M (1992) K252a is a selective inhibitor of the tyrosine protein kinase activity of the trk family of oncogenes and neurotrophin receptors. Oncogene 7:371–381
21. Roux PP, Dorval G, Boudreau M, Angers-Loustau A, Morris SJ, Makkerh J, Barker PA (2002) K252a and CEP1347 are neuroprotective compounds that inhibit mixed-lineage kinase-3 and induce activation of Akt and ERK. J Biol Chem 277:49473–49480
22. Perez-Pinera P, Hernandez T, Garcia-Suarez O, de Carlos F, Germana A, Del Valle M, Astudillo A, Vega JA (2007) The Trk tyrosine kinase inhibitor K252a regulates growth of lung adenocarcinomas. Mol Cell Biochem 295:19–26

23. Morotti A, Mila S, Accornero P, Tagliabue E, Ponzetto C (2002) K252a inhibits the oncogenic properties of Met, the HGF receptor. Oncogene 21:4885–4893
24. Takai N, Ueda T, Nishida M, Nasu K, Narahara H (2008) K252a is highly effective in suppressing the growth of human endometrial cancer cells, but has little effect on normal human endometrial epithelial cells. Oncol Rep 19:749–753
25. Takai N, Ueda T, Nishida M, Nasu K, Fukuda J, Miyakawa I (2005) K252a inhibits proliferation of ovarian cancer cells by upregulating p21WAF1. Oncol Rep 14:141–143
26. Illmer T, Ehninger G (2007) FLT3 kinase inhibitors in the management of acute myeloid leukemia. Clin Lymphoma Myeloma 8(Suppl 1):S24–S34
27. Zacchigna S, Lambrechts D, Carmeliet P (2008) Neurovascular signalling defects in neurodegeneration. Nat Rev Neurosci 9:169–181
28. Lecht S, Arien-Zakay H, Marcinkiewicz C, Lelkes PI, Lazarovici P (2009) Nerve growth factor-induced protection of brain capillary endothelial cells exposed to oxygen-glucose deprivation involves attenuation of Erk phosphorylation. J Mol Neurosci doi: 10.1007/s12031-12009-19318-12030
29. Arien-Zakay H, Lecht S, Perets A, Roszell B, Lelkes PI, Lazarovici P (2009) Quantitative assessment of neuronal differentiation in three-dimensional collagen gels using enhanced green fluorescence protein expressing PC12 pheochromocytoma cells. J Mol Neurosci 37:225–237
30. Arien-Zakay H, Lecht S, Bercu MM, Tabakman R, Kohen R, Galski H, Nagler A, Lazarovici P (2008) Neuroprotection by cord blood neural progenitors involves antioxidants, neurotrophic and angiogenic factors. Exp Neurol 216:83–94
31. Lelkes PI, Hahn KA, Karmiol S, Schmidt DH (1998) Hypoxia/reoxygenation enhances tube formation of cultured human microvascular endothelial cells: role of reactive oxygen species. In: Maragoudakis ME (ed) Angiogenesis. Plenum Press, New York and London
32. Papadimitriou E, Unsworth BR, Maragoudakis ME, Lelkes PI (1993) Time course and quantitation of extracellular matrix maturation in the chick chorioallantoic membrane and in cultured endothelial cells. Endothelium 1:207–219
33. Mizuguchi H, Hashioka Y, Fujii A, Utoguchi N, Kubo K, Nakagawa S, Baba A, Mayumi T (1994) Glial extracellular matrix modulates gamma-glutamyl transpeptidase activity in cultured bovine brain capillary and bovine aortic endothelial cells. Brain Res 651:155–159
34. Kohan M, Bader R, Puxeddu I, Levi-Schaffer F, Breuer R, Berkman N (2007) Enhanced osteopontin expression in a murine model of allergen-induced airway remodelling. Clin Exp Allergy 37:1444–1454
35. Omidi Y, Campbell L, Barar J, Connell D, Akhtar S, Gumbleton M (2003) Evaluation of the immortalised mouse brain capillary endothelial cell line, b.End3, as an in vitro blood-brain barrier model for drug uptake and transport studies. Brain Res 990: 95–112
36. Katzir I, Shani J, Regev K, Shabashov D, Lazarovici P (2002) A quantitative bioassay for nerve growth factor, using PC12 clones expressing different levels of trkA receptors. J Mol Neurosci 18:251–264
37. Lecht S, Foerster C, Arien-Zakay H, Marcinkiewicz C, Lazarovici P, Lelkes PI (2009) Cardiac microvascular endothelial cells express and release nerve growth factor but not fibroblast growth factor-2. In Vitro Cell Dev Biol Anim doi:10.1007/s11626-11009-19267-11625
38. Kim H, Li Q, Hempstead BL, Madri JA (2004) Paracrine and autocrine functions of brain-derived neurotrophic factor (BDNF) and nerve growth factor (NGF) in brain-derived endothelial cells. J Biol Chem 279:33538–33546
39. Kaplan DR, Miller FD (2000) Neurotrophin signal transduction in the nervous system. Curr Opin Neurobiol 10:381–391
40. Ohmi K, Yamashita S, Hashimoto Y, Nonomura Y (1993) Induction of giant endothelial cells in culture by K-252a, a protein kinase inhibitor. Jpn J Pharmacol 63:195–202
41. Vaudry D, Stork PJ, Lazarovici P, Eiden LE (2002) Signaling pathways for PC12 cell differentiation: making the right connections. Science 296:1648–1649
42. Hartmann C, Zozulya A, Wegener J, Galla HJ (2007) The impact of glia-derived extracellular matrices on the barrier function of cerebral endothelial cells: an in vitro study. Exp Cell Res 313:1318–1325
43. Grant DS, Lelkes PI, Fukuda K, Kleinman HK (1991) Intracellular mechanisms involved in basement membrane induced blood vessel differentiation in vitro. In Vitro Cell Dev Biol 27A:327–336
44. Papadimitriou E, Waters CR, Manolopoulos VG, Unsworth BR, Maragoudakis ME, Lelkes PL (2001) Regulation of extracellular matrix remodeling and MMP-2 activation in cultured rat adrenal medullary endothelial cells. Endothelium 8:181–194
45. Utoguchi N, Ikeda K, Saeki K, Oka N, Mizuguchi H, Kubo K, Nakagawa S, Mayumi T (1995) Ascorbic acid stimulates barrier function of cultured endothelial cell monolayer. J Cell Physiol 163:393–399
46. Ashino H, Shimamura M, Nakajima H, Dombou M, Kawanaka S, Oikawa T, Iwaguchi T, Kawashima S (2003) Novel function of ascorbic acid as an angiostatic factor. Angiogenesis 6:259–269
47. Moser KV, Reindl M, Blasig I, Humpel C (2004) Brain capillary endothelial cells proliferate in response to NGF, express NGF receptors and secrete NGF after inflammation. Brain Res 1017: 53–60
48. Andjelkovic AV, Stamatovic SM, Keep RF (2003) The protective effects of preconditioning on cerebral endothelial cells in vitro. J Cereb Blood Flow Metab 23:1348–1355
49. Thijssen VL, van Beijnum JR, Mayo KH, Griffioen AW (2007) Identification of novel drug targets for angiostatic cancer therapy; it takes two to tango. Curr Pharm Des 13:3576–3583
50. Satoh M, Kokubu N, Matsuo K, Takayanagi I (1995) Alpha 1A-adrenoceptor subtype effectively increases Ca(2+)-sensitivity for contraction in rabbit thoracic aorta. Gen Pharmacol 26:357–362
51. Ohmi K, Yamashita S, Nonomura Y (1990) Effect of K252a, a protein kinase inhibitor, on the proliferation of vascular smooth muscle cells. Biochem Biophys Res Commun 173:976–981
52. Miura S, Matsuo Y, Saku K (2004) Simvastatin suppresses coronary artery endothelial tube formation by disrupting Ras/Raf/ERK signaling. Atherosclerosis 175:235–243
53. Yang YH, Wang Y, Lam KS, Yau MH, Cheng KK, Zhang J, Zhu W, Wu D, Xu A (2008) Suppression of the Raf/MEK/ERK signaling cascade and inhibition of angiogenesis by the carboxyl terminus of angiopoietin-like protein 4. Arterioscler Thromb Vasc Biol 28:835–840
54. Tabruyn SP, Griffioen AW (2007) Molecular pathways of angiogenesis inhibition. Biochem Biophys Res Commun 355:1–5
55. Ali AS, Ali S, El-Rayes BF, Philip PA, Sarkar FH (2009) Exploitation of protein kinase C: a useful target for cancer therapy. Cancer Treat Rev 35:1–8
56. Grothey A, Galanis E (2009) Targeting angiogenesis: progress with anti-VEGF treatment with large molecules. Nat Rev Clin Oncol 6:507–518
57. Abdiche YN, Malashock DS, Pons J (2008) Probing the binding mechanism and affinity of tanezumab, a recombinant humanized anti-NGF monoclonal antibody, using a repertoire of biosensors. Protein Sci 17:1326–1335
58. Wilhelm S, Carter C, Lynch M, Lowinger T, Dumas J, Smith RA, Schwartz B, Simantov R, Kelley S (2006) Discovery and development of sorafenib: a multikinase inhibitor for treating cancer. Nat Rev Drug Discov 5:835–844

59. Faivre S, Demetri G, Sargent W, Raymond E (2007) Molecular basis for sunitinib efficacy and future clinical development. Nat Rev Drug Discov 6:734–745
60. Quintas-Cardama A, Cortes J (2008) Nilotinib: a phenylamino-pyrimidine derivative with activity against BCR-ABL, KIT and PDGFR kinases. Future Oncol 4:611–621
61. Festuccia C, Muzi P, Gravina GL, Millimaggi D, Speca S, Dolo V, Ricevuto E, Vicentini C, Bologna M (2007) Tyrosine kinase inhibitor CEP-701 blocks the NTRK1/NGF receptor and limits the invasive capability of prostate cancer cells in vitro. Int J Oncol 30:193–200